Design principles for thrust enhancement in shape-changing AUVs

F. Giorgio-Serchi and G. D. Weymouth
University of Southampton

ABSTRACT: Marine operations are in growing demand of robust, autonomous and highly manoeuvrable unmanned systems in order to foster the degree of automation in the offshore and maritime sectors. One way to address these needs is to adopt innovative design principles where thrust-augmenting strategies are coupled with structurally-compliant technologies. With this purpose in mind, we have studied the capability of aquatic pulsed-jetting bodies to boost thrust generation by altering their external body-shape. Given the complex hydroelastic response of these kind of vehicles to their actuation, we devise an analytical model to effectively predict their unsteady dynamics for design and control purposes. This model is validated against the speed and mass variation from recent experiments and provides an accurate estimate of the contribution of external added-mass variation to total jetting thrust. These results pave the way to our preliminary development of a new kind of soft-bodied aquatic vehicle capable of fully exploiting the benefit from added-mass variation effects for the purpose of sustained self-propulsion.

1 INTRODUCTION

1.1 Underwater robotics

The maritime sector requires complex tasks to be performed in always more forbidding environments and with a constantly increasing degree of autonomy. These requirements are fostering the incremental improvement of the manoeuvring capabilities of state-of-the-art underwater vehicles (Vaganay et al., 2009; Elvander and Hawkes, 2012; Vasilescu et al., 2010) either by refining navigation and positioning systems (see Hover et al., 2012) or by undertaking completely disruptive design processes. This is the case of biomimetics, where water dwelling organisms are taken as the source of inspiration for the development of innovative vehicles.

Underwater robotics has extensively employed the swimming biomechanics of fish and other aquatic creatures in order to endow new prototypes with the capability of hovering, short radius turning, fast start/slowdown and low-speed manoeuvring (Licht et al., 2004; Yu et al., 2012; Colgate and Lynch, 2004). The propulsion routines of biologically-inspired robots entails, for the most part, cyclic oscillations of one or more body parts. These commonly drive the onset of momentum-rich vortical flow structures responsible for generating unsteady hydrodynamical forces which propel the vehicles. Flapping foil propulsion, for instance, relies on actuators which mimic the continuous deformation of fins and tails by means of discrete sequences of rigid links and joints. However, new actuators which more closely resemble the compliant nature of leaving tissues are now being developed by exploiting soft structures (Marchese et al., 2014) which offer the advantage of intrinsic safer physical interaction with the environment as well as a higher degree of agility (Wang and Iida, 2015; Woodman et al., 2012; Mortl et al., 2012).

1.2 Aquatic volume-changing vehicles

The employment of compliant body parts or entirely soft-bodied vehicles and actuators not only provides a higher degree of structural resilience and the need for less-refined control strategies, but it also lends itself to mimic those organisms which rely extensively on large body-volume variations to propel themselves, such as squids and octopi. These sea-dwelling creatures sport a repertoire of extremely aggressive manoeuvres thanks to their pulsed-jetting propulsion which is driven by the inflation and deflation of a cavity of their body (Johnson, et al. 1972). While the study on pulsed-jet locomotion has mainly revolved around the contribution to thrust from the vortex generated at the nozzle exit-plane (Krieg & Mohseni, 2013), it is becoming apparent that the role of the external shape variation represents a prominent factor in this mode of propulsion, (Weymouth & Triantafyllou, 2013; Giorgio-Serchi & Weymouth, 2016). The analysis performed on submerged bodies subject to abrupt shape-changes confirms that the forces associated with added-mass variation participate in the generation of thrust to a large extent, (Weymouth et al., 2015; Giorgio-Serchi & Weymouth, 2016). Thus, the exploitation of added-mass variation as a

potential source of thrust can have a major impact on the design (Giorgio-Serchi et al., 2016) and control (Giorgio-Serchi et al., 2015; Renda et al., 2015) of new kinds of underwater vehicles. To this end, in this paper we devise a model for capturing the coupled fluid-structure-interaction effects of such kind of vehicles. The purpose of this model is to offer a fast tool for exploring the design space of new prototypes and shed light over the potential to employ added-mass variation effect as a source of thrust in aquatic vehicles.

2 VEHICLE DESIGN

2.1 Propulsion routine

Our purpose is to develop a new soft aquatic prototype which is capable of performing a repetitive sequence of pulsed-jets by means of its own body-shape variation. The mode of actuation of the vehicle must exploit thrust generated both by the expulsion of mass and by the variation of added mass. In order for this to happen, the vehicle must be capable of undergoing volume variations while at the same time maintaining a shape as streamlined as possible throughout each single cycle of pulsation.

2.2 Actuation

Based on these requirements, the generic outline of the vehicle entails a hollow shell of elastic rubber-like material with two nozzles. At the bow of the vehicle, a secondary nozzle enables the inflow from ambient fluid. This process, mediated by a pump, accounts for the displacement of fluid into the shell, thus driving its inflation. At the stern, the principal nozzle regulates the outflow from within the cavity by means of a controlled valve. This working principle entails the following routine:

- activate the pump while the principal nozzle is sealed by the valve,
- inflate the shell, thus increasing its elastic potential energy,
- deactivate the pump and open the valve of the principal nozzle thus enabling the deflation of the shell and hence the expulsion of a finite slug of fluid.

In order to maximize the thrust output the contributions from mass expulsion and external added-mass variation must be carefully studied. However, since the body deformation of the vehicle plays such a crucial part in determining the total jetting force (i.e. the sum of the momentum of the issuing fluid and the added-mass variation effect), in studying the dynamics of this vehicle we must account for the highly non-linear coupled fluid-structure effects.

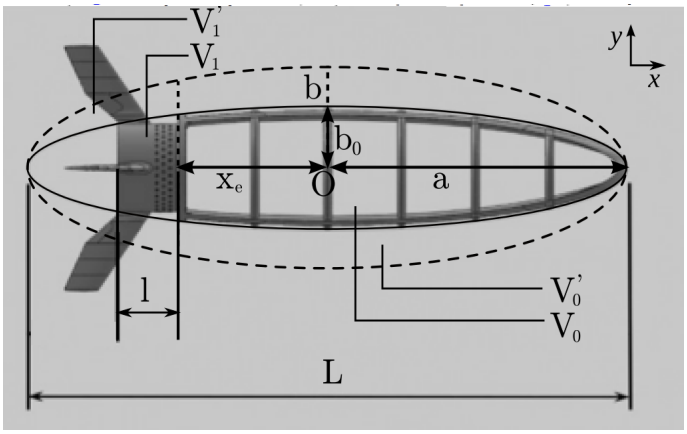

Figure 1: schematic of the shape-changing jet-propelled vehicle, modified from Weymouth et al. (2015).

3 VEHICLE MODELLING

3.1 Model overview

The model consists of a coupled system describing the rigid body dynamics of a hollow ellipsoid of revolution unsteadily translating in a quiescent fluid due to the deformations of its body. The deformation of the body, which regulates the generation of thrust, depends on the dynamics of the shell, which in turns is affected by fluid terms internal and external to the cavity.

The description of the shell accounts for the deformation of an ellipsoid of revolution by focusing on the dynamics of its minor-semi-axis. This enables to treat the body-shape variation of the ellipsoid as a 1d structural model where solid and fluid terms are lumped together. This model accounts for the inertial contribution from the fluid internal to the cavity as it deforms while at the same time uses an ensemble elastic constant to characterize the stiffness of the body. The contribution from the external fluid on the dynamics of the shell is embodied by a ”fluid stiffness” term which depends on the external shape of the ellipsoid and its translational velocity and affects the deformation of the cavity by enhancing its structural stiffness.

3.2 Rigid body model

The translation dynamics of the body is modelled as:

$$\left(M+m_{\ddot{x}}+m_f\right)\ddot{x}+\tau+\frac{1}{2}\rho C_d A\,\dot{x}\left|\dot{x}\right|+\dot{m}_{\ddot{x}}\,\dot{x}=0 \qquad (1)$$

Here M is the solid mass of the shell, $m_{\ddot{x}}(t)$ is the time-varying added-mass of an ellipsoid of revolution, $m_f(t)$ is the time-varying mass of fluid inside the shell, τ is the thrust of the pulsed-jetting routine, A is the cross section of the ellipsoid. The

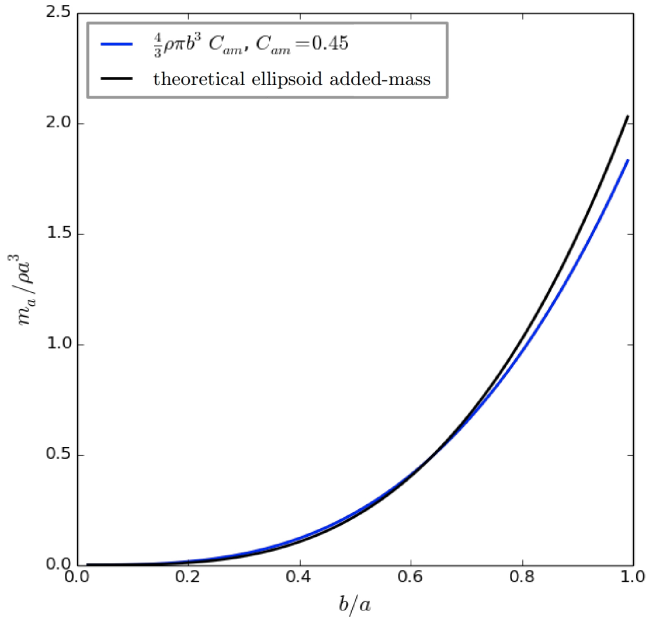

Figure 2: comparison between exact added mass formulation for an ellipsoid of revolution (black) as derived by Sedov (Korotkin, 2009) and that obtained with the simplified form of eq. (2), (blue).

thrust term is clearly linked to the deformation of the cavity. In addition, we account for the added-mass variation effect associated with the shape change of the vehicle as it translates in water, which further contributes to the thrust force.

Having defined *a*, *b*, b_0 , Δb, ρ, ρ_s respectively as the major semi-axis, the minor semi-axis, the minor semi-axis in its unstrained state, the shell thickness the fluid density and the density of the solid, see Fig. 1, these are respectively defined as follows:

$$M=\frac{4}{3}\pi a\Delta b$$

$$m_{\ddot{x}}(t)=\frac{4}{3}\pi b(t)^3 C_{\ddot{x}} \qquad (2)$$

$$m_f(t)=\frac{4}{3}\pi a b(t)^2-\pi\int_{x_e}^{a} b^2\left[1-\left(\frac{x}{a}\right)^2\right]dx$$

$$\tau=\frac{\dot{m}_f^2}{\rho\pi r_0^2}$$

$$\dot{m}_{\dot{x}}(t)=4\pi\rho b^2\dot{b}$$

where $m_f(t)$ is obtained by subtracting the volume V_0' (see Fig. 1) from the total volume in order to account for V_0' alone. Here we make use of a simplified definition for the added mass derived by Sedov (see Korotkin, 2009). The form of $m_{\ddot{x}}(t)$ in eq.(2) is comparable to the exact potential-flow formulation for values of $0<b/a\leq 0.7$ when $C_{\ddot{x}}$ = 0.45, Fig. 2.

3.3 Elastic shell model

The elastic membrane is modelled as an ellipsoid of revolution whose inflation and deflation is regulated exclusively by a spring located at its minor-axis, see Fig. 1. This enables us to write its dynamics in the following manner:

$$\left(I_b+m_{\ddot{b}}+m_{\ddot{b}}'\right)\ddot{b}+c\dot{b}+k(b-b_0)+k_{\dot{x}}b=0 \qquad (3)$$

Here the terms I_b , $m_{\ddot{b}}$, $m_{\ddot{b}}'$, *c*, *k* and $k_{\dot{x}}$ respectively represent the effective inertia of the shell walls, the internal added-mass associated with the acceleration of fluid within the shell and within the exit tube due to squeezing *b*, the coefficient of viscous losses across the nozzle and nozzle inlet, the effective elastic constant of the shell and a "fluid stiffness" term associated with the differential pressure across the shell walls due to the external flow.

The viscous losses, expressed by coefficient *c*, are estimated based on Darcy's friction factors. The pressure head loss at the nozzle inlet and due to wall shear stresses along the nozzle can be written:

$$\Delta p=\frac{1}{2}f\rho q|q|$$

where *q* represents the flow speed across the nozzle,

$$q=\frac{\dot{m}_f}{\rho\pi r_0^2}$$

and *f* is Darcy's friction factor

$$f=\left(\frac{64}{Re}\frac{l}{2r_0}+0.5\right)$$

which comprises of the term for head loss along constant radius cylindrical pipes at *Re*<2100 and of an additional coefficient which accounts for viscous effect at square-edged inlets. This leads to the definition of the viscous term *c*,

$$c=\frac{32}{9}\left(\frac{64}{Re}\frac{l}{2r_0}+0.5\right)\frac{a^2}{\rho r_0^4}b^2|\dot{b}|$$

The remaining terms of eq. (3) are described in the following sections.

3.4 Internal added-mass: $m_{\ddot{b}}$ and $m_{\ddot{b}}'$

In order to model the inertial effect which the shell is subject to while undergoing deflation, we will model the internal energy and added mass of the shrinking ellipsoid as a 1D-flow.

$$E=\frac{1}{2}\int u^2 du\approx\frac{1}{2}\int_{-1}^{x_e}\frac{F(x)^2}{A(x)}dx \qquad (4)$$

where *F(x)* represents the flux through cross section *A(x)* and x_e <1 represents the location of the nozzle inflow plane. Here x_e is scaled with the length of the major semi-axis *a*. Given the condition

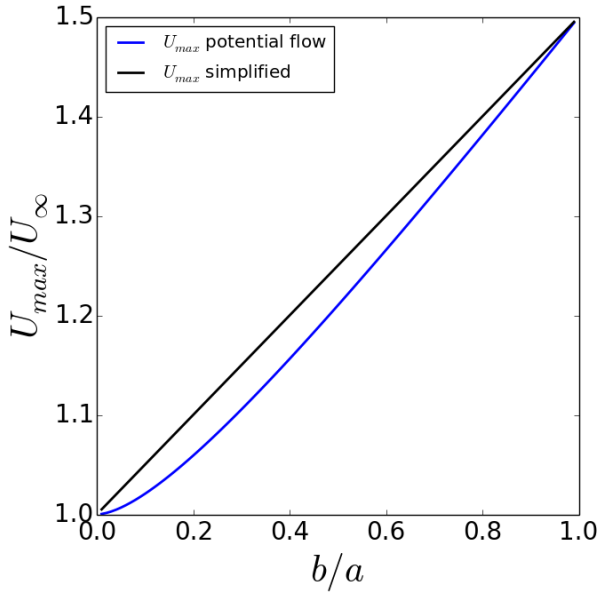

Figure 3: comparison between maximum velocity over the an ellipsoid estimated with exact potential flow solution (blue) and with the simplified formulation (black) of eq. (9).

of incompressibility, the variation in cross section due to the shrinkage of the shell must be equal to the variation of flux across that section. This implies that:

$$\frac{dF}{dx}=\dot{A}=2\pi R\dot{R}=2\pi R^2\frac{\dot{b}}{b} \tag{5}$$

where $R^2=b^2(1-x^2)$ is the section radius of the ellipsoid and its derivative is $\dot{R}=R\dot{b}/b$. By substituting these into eq.(5) and integrating along *x* we obtain:

$$F=\frac{2}{3}\pi b\dot{b}(2+3x-x^3)$$

By substituting for *F(x)* and *A(x)* in eq.(4) we obtain,

$$E=\frac{4}{9}\pi\dot{b}^2\int_{-1}^{x_e}\frac{(2+3x+x^3)}{1-x^2}dx \tag{6}$$

Since the added-mass associated with the internal flow is defined as

$$E=\frac{1}{2}m_{\ddot{b}}\dot{b}^2$$

then, by using eq.(6) and the assumption that $x_e\approx 1$,

$$\frac{m_{\ddot{b}}}{\rho a^3}=\frac{16}{9}\pi\left(2\log\left(\frac{2}{1-x_e}+x_e-\frac{34}{15}\right)\right) \tag{7}$$

Similarly, the inertial term associated with the presence of a cylindrical nozzle of finite length *l* (again scaled by the major semi-axis length *a*) can be easily derived by assuming the flow speed to be uniform, thus enabling the assumption that $F(x_e)\approx F(1)$ which yields:

$$\frac{m_{\ddot{b}}}{\rho a^3}=lA(x_e)\left(\frac{F(1)/\dot{b}}{A(x_e)}\right)^2=\frac{64}{9}\pi l\frac{1}{1-x_e^2} \tag{8}$$

3.5 Fluid stiffness: $k_{\dot{x}}$

Another term which arises due to the body translation and which affects the dynamics of the shell pulsation is the fluid stiffness. The fluid flow over the body of the vehicle is responsible for the onset of a pressure differential across the shell walls. In order to estimate the significance of this term, we consider the maximum speed over the body:

$$\frac{U_{max}}{U_\infty}=1+\frac{b}{(2a)} \tag{9}$$

This formulation approximates the exact potential flow for an axisymmetric ellipsoid, see Fig. 3. The pressure coefficient is, $C_p=1-U_{max}^2$ and the compression force on the body center-line is: $\Delta C_p=-2C_p+C_p'$ where C_p' is the internal pressure coefficient. The integral force C_F over the body can be estimated as $C_F=2\pi ab\Delta C_p$, which enables to derive an equivalent fluid restoring force under the condition that $dC_F=k_{\ddot{x}}db$. Hence by differentiating C_F about *db*, we obtain:

$$k_{\ddot{x}}=-2\pi b\left(2+\frac{3}{4}\frac{b}{a}\right) \tag{10}$$

The degree by which this term affects the dynamics of the vehicle depends on its relative magnitude with respect to the lumped elastic constant of the rubber material as discussed in section 4.2.

4 MODEL TESTING

4.1 Model parameters

The solution of the coupled system defined by eq.(1) and (3) is validated against the experimental test case of Weymouth et al. (2015). This can be solved by prescribing initial conditions *x*(0) = 0, $\dot{x}(0)=0$, *b*(0) = 0.76*L* (see Fig. 1) and $\dot{b}(0)=0$. The geometrical variables are also prescribed based on Weymouth et al. (2015) as follows: *L* = 36cm, *a* = *L*/2cm, b_0 = *a*/5cm, x_e = 0.82, *l* = 0.2 (notice that x_e and *l* are non-dimensionally defined based on *a* and their dimensional size is respectively $\tilde{x}_e$ =15cm and $\tilde{l}$ = 3.6cm) which yield r_0 = 2.2cm; Δb = 0.05 b_0 cm, and ρ = 1000 kg/m^3 . The density of the solid material is chosen equivalent to that of common rubber-like compounds, i.e. ρ_s = 1.1ρ

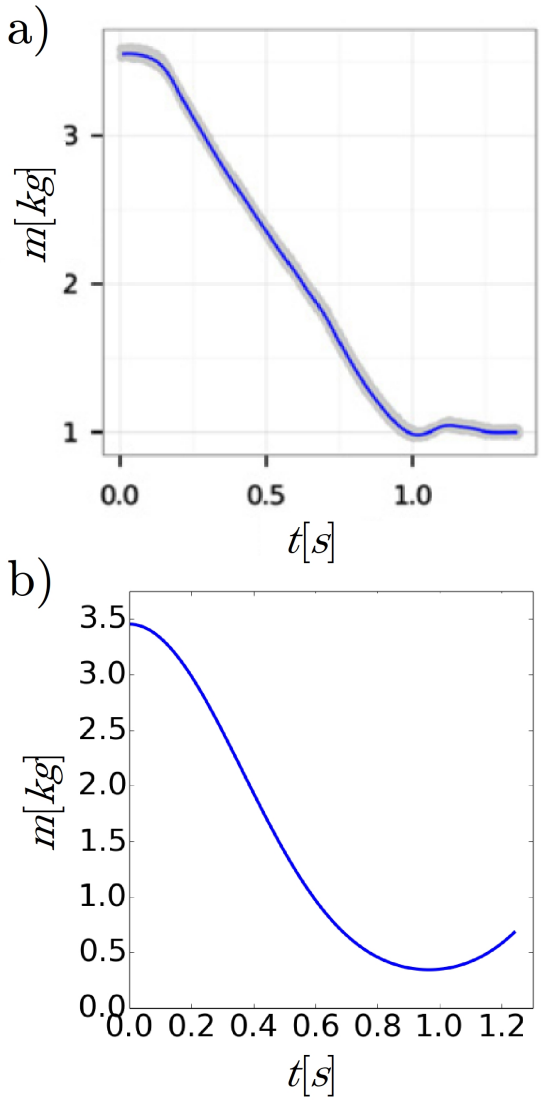

Figure 4: comparison between the experimental (a) and simulated (b) fluid mass inside the shell cavity throughout the pulsation routine.

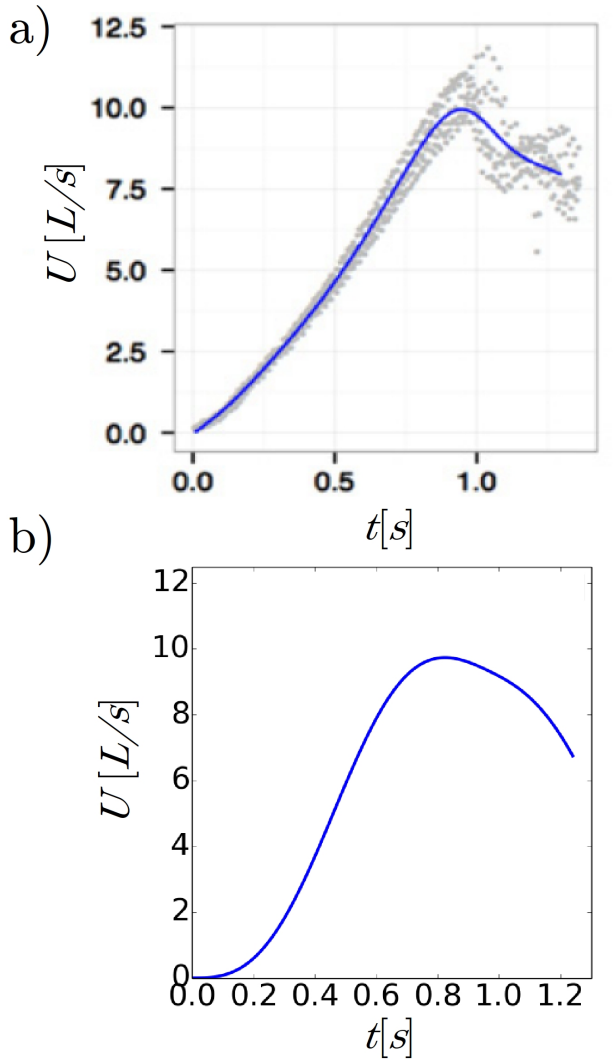

Figure 5: comparison between the experimental (a) and simulated (b) vehicle speed throughout the pulsation routine.

kg/m^3 . The drag coefficient of an ellipsoid of revolution is found to be C_d = 0.1 for 1.5< $L/2r_0$ < 8. This leaves only the stiffness of the spring to be determined empirically.

4.2 Model results

By selecting a lumped elastic constant for the shell of k = 2094N/m, a very close match with the experimental results of Weymouth et al. (2015) is achieved, see Fig. 4 and 5. The variation of fluid mass in the cavity is informative on the dynamics of the shell throughout the pulsation. The differences between the experimental Fig. 4(a) and simulated Fig. 4(b) case are motivated by the prototype comprising of a rigid endo-skeleton (see Fig. 1) which prevents the membrane from squeezing beyond the 1.0 kg limit. This not being accounted for in the model, clearly allows the shell to oscillate around the equilibrium width b_0 , point where the fluid content in the shell is about 1.0 kg. Similarly, the description of the speed of the vehicles is captured with remarkable accuracy, Fig. 5.

Having confirmed the validity of the model in capturing the dynamics of the prototype we can estimate the importance of the fluid stiffness term. By comparing the magnitude of $k_{\ddot{x}}$ with respect to k, we observe that, for the material considered in this case, the fluid restoring force is always negligible throughout the whole sequence of pulsation, see Fig. 6.

More importantly, this model enables us to estimate the role of thrust and added-mass variation effect in determining the burst of acceleration of the body. From Fig. 7, it is apparent that the contribution from added-mass variation is prominent and, in agreement with what is postulated in Weymouth et al. (2015), it accounts for as much as 75% of the propulsive force of the vehicle.

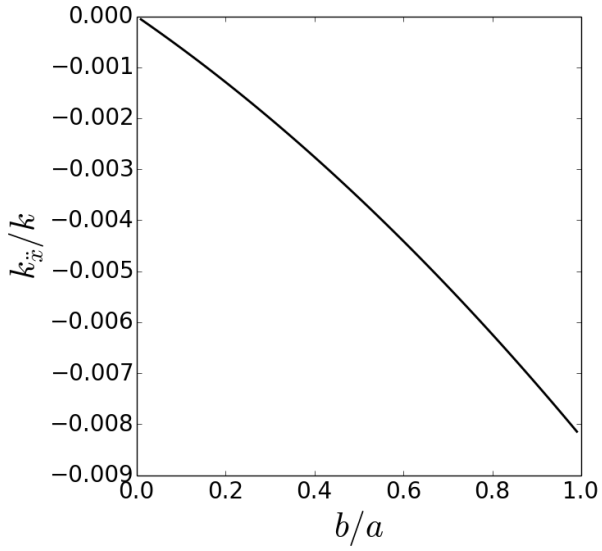

Figure 6: magnitude of the fluid stiffness relative to the lumped elastic constant of the shell at various degrees of inflation of the shell.

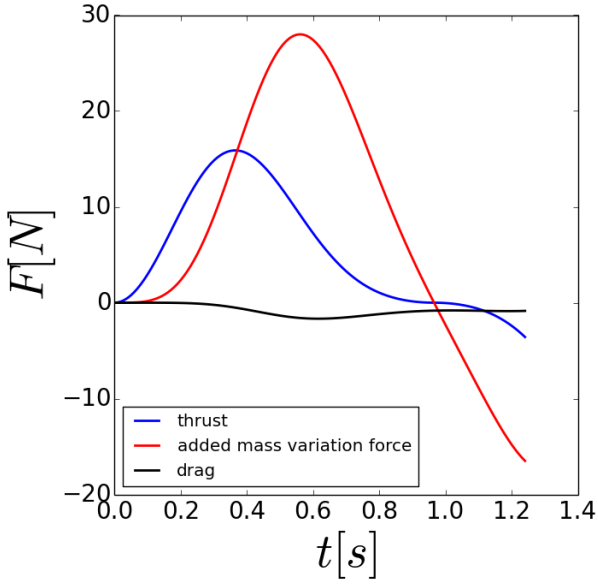

Figure 7: comparison of the relative magnitude of drag, thrust and added-mass variation force during the pulsation routine.

5 CONCLUSIONS

In order to develop a new kind of soft unmanned underwater system capable of propelling itself by exploiting pulsed-jetting and added-mass variation, we have devised a fast analytical model which captures the hydroelastic dynamics of highly deformable self-propelling aquatic bodies. The model comprises of several terms important in this mode of actuation. These include, for the internal fluid, the unsteady inertial effect due to confinement of the flow which appears to be the leading the term in regulating the shell collapse. For what concerns the fluid surrounding the body, the model incorporates the added-mass variation and a "fluid stiffness" term. In the case considered in this manuscript, it is found that added-mass variation represents 75% of the total thrust generated, while fluid restoring force participates to only about 1% of the total shell elasticity. These results lay the foundation for the preliminary design of innovative soft unmanned underwater vehicles capable of exploiting the benefit from added-mass variation for the purpose of sustained self-propulsion.

6 REFERENCES

Colgate, J. and Lynch, K. *Mechanics and control of swimming: a review.* Oceanic Engineering, IEEE Journal of, 29(3):660–673, 2004.

Elvander, J. and Hawkes, G., *Rovs and auvs in support of marine renewable technologies.* Oceans, 2012, pages 1–6.

Giorgio-Serchi, F., Arienti, A. and Laschi, C., *Underwater soft-bodied pulsed-jet thrusters: Actuator modeling and performance profiling*, International Journal of Robotics Research, 35:1308–1329, 2016. DOI: 10.1177/0278364915622569

Giorgio-Serchi, F., Renda, F., Calisti, M. and Laschi, C., *Thrust depletion at high pulsation frequencies in underactuated, soft-bodied, pulsed-jet vehicles*, in MTS/IEEE OCEANS, Genova, Italy, May 2015. DOI: 10.1109/OCEANS-Genova.2015.7271369

Giorgio-Serchi, F. and Weymouth, G. D., *Drag cancellation by added-mass pumping*, Journal of Fluid Mechanics, vol. 798, 2016. DOI: 10.1017/jfm.2016.353

Giorgio-Serchi, F., & Weymouth, G. *Underwater soft robotics, the benefit of body-shape variations in aquatic propulsion*. In *Soft Robotics: Trends, Applications and Challenges.* (pp. 37-46). (Biosystems & Biorobotics; No. 17). Cham, Springer International Publishing. DOI: 10.1007/978-3-319-46460-2_6

Hover, F. S., Eustice, R. M., Kim, A., Englot, B., Johannsson, H., Kaess, M., and Leonard, J. J. *Advanced perception, navigation and planning for autonomous in-water ship hull inspection* The International Journal of Robotics Research, 31(12):1445–1464, 2012.

Johnson W, Soden PD, Trueman ER, *A study in jet propulsion: An analysis of the motion of the squid, Loligo Vulgaris*. Journal of Experimental Biology 56: 155–165, 1972.

Korotkin, A. I., *Added mass of ship structures*, Springer Series of Fluid Mechanicsand its applications, Springer Netherlands, vol. 1, 2009.

Licht, S., Polidoro, V., Flores, M., Hover, F., and Triantafyllou, M. *Design and projected performance of a flapping foil auv.* Oceanic Engineering, IEEE Journal of, 29(3):786–794, 2004.

Marchese, A. D., Onal Cagdas, D., and Rus, D. *Autonomous soft robotic fish capable of escape maneuvers using fluidic elastomer actuators*. Soft Robotics, 1(1):75–673, 2014.

Mortl, A., Lawitzky, M., Kucukyilmaz, A., Sezgin, M., Basdogan, C., and Hirche, S. *The role of roles: Physical cooperation between humans and robots.* The International Journal of Robotics Research, 31, 13, 1656-1674, 2012.

Renda, F., Giorgio-Serchi, F., Boyer, F. and Laschi, C., *Modelling cephalopod-inspired pulsed-jet locomotion for underwater soft robots*, Bioinspiration & Biomimetics, vol. 10(5), 1-12, 2015. DOI: 10.1088/1748-3190/10/5/055005

Krieg, M., and Mohseni, **K.,** *Modelling circulation, impulse and kinetic energy of starting jets with non-zero radial velocity*, Journal of Fluid Mechanics, vol. 79, pp. 488–526, 2013.

Vaganay, J., Gurfinkel, L., Elkins, M., Jankins, D., and Shurn, K.. *Hovering autonomous underwater vehicle-system design improvements and performance evaluation results.* In UUST, International Symposium on Unmanned Untethered Submarine Technology, 2009.

Vasilescu, I., Detweiler, C., Doniec, M., Gurdan, D., Sosnowski, S., Stumpf, J., and Rus, D. *Amour v: a hovering energy efficient underwater robot capable of dynamic payloads*, The International Journal of Robotics Research, 29(5):547-570, 2010.

Yu, J., Ding, R., Yang, Q., Tan, M., Wang, W., and Zhang, J. *On a bio-inspired amphibious robot capable of multimodal motion*. Mechatronics, IEEE/ASME Transactions on, 17(5):847–856, 2012.

Woodman, R., Winfield, A., Harper, C., and Fraser, M. *Building safer robots: Safety driven control*. The International Journal of Robotics Research, 31, 13, 1603-1626, 2012.

Weymouth, G. D. and Triantafyllou, **M.,** *Ultra-fast escape of a deformable jet-propelled body,* Journal of Fluid Mechanics, vol. 721, pp. 367–385, 2013.

Weymouth, G.D., Subramaniam, V. and Triantafyllou, M., *Ultra-fast escape maneuver of an octopus-inspired robot*, Bioinspiration & Biomimetics, 10, 016016, 2015.